Iris Crypts Influence Dynamic Changes of Iris Volume

Jacqueline Chua, PhD,[1,2] Sri Gowtham Thakku, BEng,[1] Tin A. Tun, MD,[1] Monisha E. Nongpiur, MD, PhD,[1,2] Marcus Chiang Lee Tan, MBBS,[1] Michael J.A. Girard, PhD,[1,3] Tien Yin Wong, FRCS, PhD,[1,2,4] Joanne Hui Min Quah, MMed,[5] Tin Aung, FRCS, PhD,[1,2,4] Ching-Yu Cheng, MD, PhD[1,2,4]

Purpose: To determine the association of iris surface features with iris volume change after physiologic pupil dilation in adults.

Design: Cross-sectional observational study.

Participants: Chinese adults aged $\geq$ 50 years without ocular diseases.

Methods: Digital iris photographs were taken from eyes of each participant and graded for crypts (by number and size) and furrows (by number and circumferential extent) following a standardized grading scheme. Iris color was measured objectively, using the Commission Internationale de l'Eclairage (CIE) L* color parameter (higher value denoting lighter iris). The anterior segment was imaged by swept-source optical coherence tomography (SS-OCT) (Casia; Tomey, Nagoya, Japan) under bright light and dark room conditions. Iris volumes in light and dark conditions were measured with custom semiautomated software, and the change in iris volume was quantified. Associations of the change in iris volume after pupil dilation with underlying iris surface features in right eyes were assessed using linear regression analysis.

Main Outcome Measures: Iris volume change after physiologic pupil dilation from light to dark condition.

Results: A total of 65 Chinese participants (mean age, 59.8±5.7 years) had gradable data for iris surface features. In light condition, higher iris crypt grade was associated independently with smaller iris volume (β [change in iris volume in millimeters per crypt grade increment] = −1.43, 95% confidence interval [CI], −2.26 to −0.59; P = 0.001) and greater reduction of iris volume on pupil dilation (β [change in iris volume in millimeters per crypt grade increment] = 0.23, 95% CI, 0.06−0.40; P = 0.010), adjusting for age, gender, presence of corneal arcus, and change in pupil size. Iris furrows and iris color were not associated with iris volume in light condition or change in iris volume (all P > 0.05).

Conclusions: Although few Chinese persons have multiple crypts on their irides, irides with more crypts were significantly thinner and lost more volume on pupil dilation. In view that the latter feature is known to be protective for acute angle-closure attack, it is likely that the macroscopic and microscopic composition of the iris is a contributing feature to angle-closure disease. *Ophthalmology 2016;123:2077-2084 © 2016 by the American Academy of Ophthalmology.*

Supplemental material is available at www.aaojournal.org.

Chinese and East Asians have a higher risk of developing primary angle-closure glaucoma (PACG), a major cause of blindness.[1] There is increasing evidence that the iris plays a crucial pathophysiologic role in the development of angle closure and PACG. Irides that are more voluminous (e.g., thicker, larger, and more convex) are associated with angle closure.[2–4] In addition to the anatomic characteristics, the physiologic dynamic responses of the iris during pupil dilation have been implicated in PACG.[5–11] By using anterior-segment optical coherence tomography (AS-OCT) imaging, eyes with previous acute angle-closure attacks do not lose as much iris volume during pupil dilation as that of healthy eyes.[5,6,11]

In addition to the angle-closure disease status, studies have found ethnicity-related factors affecting the dynamic response of the iris. Aptel and Denis[6] observed that patients with brown irides have a smaller change in iris volume on pupil dilation than those with blue irides. Consistent with this, a multiethnic study reported that persons of Chinese ethnicity with relatively less loss of the iris area were more likely to have angle closure than persons of other ethnicity.[8] In addition to ethnic difference in iris color, there is increasing evidence that Asians have fewer iris crypts compared with Europeans.[12,13] Thus, a better understanding of the iris surface features (crypts, furrows, color) and its relationship with iris volume changes may uncover important insights into the ethnic variability in the pathogenesis and risk for PACG.

We recently developed a standardized grading system to assess iris surface features in Asian eyes and reported that

irides with darker color and fewer crypts were associated with greater iris thickness[14] and narrower anterior chamber angle width.[15] We hypothesized that irides with the poorest fluid movement between iris stroma and anterior chamber, that is, the worst ability to lose fluid with dilation, will have fewer crypts, more extensive furrows, and darker color. Therefore, the change in iris volume from light to dark conditions might differ by the number and size of iris crypts, and by the number and circumferential extent of iris furrows. In this study, we determined the association between these iris surface features (crypts, furrows, and color) and the dynamic change in iris volume as measured by swept-source optical coherence tomography (SS-OCT) at different states of physiologic pupil dilation (light and dark conditions) in Chinese persons.

Methods

Participants

Subjects of this study were enrolled from a large community-based study that was conducted between June and September of 2013, which involved more than 2000 volunteers aged 50 years or older who underwent a standardized eye examination at a community polyclinic.[16] At the time of enrollment, individuals visited the polyclinic for minor health issues (nonocular) and did not have any ophthalmic symptoms at the time of consultation. A total of 300 of the participants with no history of ocular disease and normal ocular findings on the basis of eye examination (see details below) were subsequently referred back to Singapore Eye Research Institute for a follow-up eye examination that was conducted between June 2013 and August 2014. Because the aim of the larger study was to evaluate the prevalence of ocular abnormalities in older patients seeking outpatient medical care in Singapore, 300 participants who had normal findings were requested to return for a standard automated perimetry and a dilated examination (which were not performed during the polyclinic visit). For this study, we prospectively recruited 86 consecutive participants from among the participants who attended the follow-up examination between June and August 2014 for SS-OCT imaging (see later section).

Examination Procedures

After an interview to obtain demographic information and medical and ophthalmic history, each participant underwent standardized eye examination including tests for visual acuity measurement using a logarithm of the minimum angle of resolution (logMAR) chart (The Lighthouse, New York, NY), intraocular pressure measurement using noncontact tonometry, automated refraction to assess refractive error, iris photography (see later section), slit-lamp (Haag-Streit, Bern, Switzerland) examination of the anterior segment, gonioscopy, and optic disc examination through an undilated pupil by a study ophthalmologist.

Subjects were considered to have normal findings if they had presenting logMAR visual acuity (VA) of 0.3 (20/40) or better in either of the eyes, absence of ocular conditions such as angle-closure diseases, glaucoma,[17] cataract (any Lens Opacities Classification System II grading >2), and retinal or ocular comorbid conditions including, but not limited to, diabetic retinopathy and age-related macular degeneration. The study was approved by the SingHealth Centralised Institutional Review Board and conformed to the tenets of the Declaration of Helsinki. Written informed consent was obtained from all participants.

Iris Photography and Grading

Color photographs of both eyes' irides were taken using an iris imaging system (MEC-5-ASL-D7100-N85, Miles Research, Escondido, CA) that consisted of a 24-megapixel Nikon Camera (Nikon D7100, Nikon, Tokyo, Japan), a Nikon 85-mm macro lens (Nikon D3200, Nikon), an adjustable side lighting illuminator (MEC-5-ASL, Miles Research), and a chinrest/camera support (CRCS-FH4, Miles Research). Photographs were taken in a room where room fluorescent lighting was kept on. Biometric coaxial illuminators were angled 60° and used to deliver light to the iris at a constant temperature to maintain color and brightness. The camera setting was kept constant at aperture priority dial, aperture stop (*f*18), shutter speed (1/60″), ISO (200), flash power (1/2), and focal length (1 ft/0.286 m). For the purpose of grading photographs were viewed on a 1366×768/60 Hz resolution screen, using the viewing software ACDSee Photo Manager Version 11.0 (ACD Systems, Seattle, WA).

We graded iris crypts and furrows as described previously (Fig 1, available at www.aaojournal.org).[14] In brief, irides were given an integer grade between 1 and 5 based on the number and size of crypts present as follows: grade 1 (no crypts); grade 2 (1−3 crypts); grade 3 (at least 4 crypts ≤1 mm in diameter); grade 4 (at least 4 crypts >1 mm in diameter); and grade 5 (numerous crypts >1 mm in diameter, covering nearly the entire iris). Furrows were given an integer grade between 1 and 3 based on the number and circumferential extent: Grade 1 (no furrows); grade 2 (5 furrows or fewer present, extending ≤180°); and grade 3 (5 furrows or more present, extending ≥180°).

To objectively determine the iris color on the basis of iris photographs, we used the L*a*b* (LAB) color system, which was established by the Commission Internationale de l'Eclairage (CIE). Color was quantified using the digit output of L* color parameter, which measured iris reflectance or lightness—with values ranging from 0 to 100, where the higher L* value denotes lighter iris color (a value of 100 corresponds to perfect white and that of zero to black). The lightness variable L* has been used in the quantification of skin color[18−20] and has been shown to correlate with melanin content.[19,20] Iris color was determined from the middle region of the iris, where it was less affected by conditions such as corneal arcus or eyelid occlusion. A color intensity threshold was subsequently applied on the iris photograph to remove distortions, such as shadows from crypts and reflections. A custom program written using MATLAB (MathWorks Inc, Natick, MA) was used to identify the precise middle region of the iris before measuring L* (Fig 2, available at www.aaojournal.org).

Swept-Source Optical Coherence Tomography Imaging

The study participants underwent imaging using the SS-OCT (Casia SS-1000 OCT; Tomey, Nagoya, Japan), before any contact procedure or eye drops, under standardized illumination conditions as detailed next. To avoid eyelid artifact, the operator opened both eyelids, avoiding inadvertent pressure on the globe during scanning. Participants were directed toward an internal fixation target, and each eye was scanned with the 3-dimensional (3D) angle analysis scan (which takes 2.4 seconds) using the auto-alignment function. A volume scan comprising 128 radial scans, each 16 mm in length and 6 mm in depth, was used to image the iris and anterior chamber. Each image was averaged automatically from 3 consecutive scans by the algorithm native to the Casia system. All eyes were first imaged in the dark and followed by light

condition with a time difference of 2 minutes between dark and light conditions. During the dark condition, room lights were off, and no stray light was allowed in either eye. The light condition included both room fluorescent lighting on and a bright flashlight directed at the fellow (nonimaged) eye during imaging.

A single observer (TAT) used the 360° SS-OCT viewer (version 6.0; Tomey, Nagoya, Japan) to analyze 8 of 128 frames (16 anterior chamber angles, 22.5 degree increments) from a single 3D angle analysis SS-OCT scan of each eye. The only user input was to mark the scleral spur location (defined as the inward protrusion of the sclera where a change in curvature of the corneo-scleral interface was noted). After the grader marked the scleral spurs of 8 frames per scan, we used the built-in SS-OCT software, which automatically computed the angle opening distance (AOD) (750 μm). The average of the quadrants was calculated for the parameter.[21] The AOD was the length of a line from the anterior iris to the corneal endothelium perpendicular to a line drawn along the trabecular meshwork 750 μm from the scleral spur.[22] Among the various AS-OCT parameters, AOD 750 μm has been shown to have the highest diagnostic performance for identifying individuals with gonioscopic narrow angles.[23] The algorithm may be subjected to segmentation error, defined as the incorrect identification of the anterior iris boundary (~10% subjectively assessed by S.G.T.) when detecting the edges, and these segmentation errors were manually corrected by the grader. A previous study has demonstrated that measurement of AOD[21,24] and iris volume[9] with the anterior segment SS-OCT was reproducible.

Measurement of Iris Volume

We developed a customized program using MATLAB to measure iris volume automatically from SS-OCT scans. The method involved 3 steps: (1) exporting scan images from Casia and correcting for the effect of refraction in each B-scan; (2) detecting the anterior and posterior iris boundaries and their termination points in each B-scan; (3) reconstructing the iris on the basis of the boundaries detected on 128 B-scans and measuring the volume enclosed by it. Although the in-built SS-OCT software on Casia does allow us to measure iris volume, it requires manual marking of the scleral spur before any volume measurement can be made. The advantage of using MATLAB was that our program did not require manual marking of the scleral spur. A previous study has shown that measurements of iris volume are not affected significantly by changes in position of the marked scleral spur.[25] Manually marking the scleral spur on 128 B-scans for each eye in each lighting condition can be time-consuming, and using a customized program on MATLAB allowed us to calculate iris volume more quickly, without losing accuracy.

For each of the 128 cross-sections comprising 1 SS-OCT scan, the anterior and posterior boundaries of the iris were detected using a gradient-based thresholding algorithm. The anterior iris boundary was detected as the anterior chamber−anterior iris surface interface, whereas the posterior iris boundary was detected as the external border of the iris pigment epithelium (Fig 3, available at www.aaojournal.org).

The termination points of these boundaries were defined by the pupillary ruff at the pupillary end and the iris root at the ciliary end. Algorithmically, the pupillary ruff was identified as the point with a sharp change in intensity gradient in the horizontal direction; the iris root, defined as the point where the iris and ciliary boundaries meet, was identified using the anterior iris boundary and based on a sharp change in horizontal intensity gradient (appropriate for closed angles) or the point where the boundary curved back up (appropriate for open angles); of these 2 candidate points, the one farther away from the pupil center was chosen.

Once the iris boundaries were identified on all 128 cross-sections, a 3D reconstruction of the entire iris was generated to allow for measurement of iris volume and visualization of the iris surface (Fig 4, available at www.aaojournal.org). On the basis of this reconstruction, iris volume was defined as the volume enclosed by the space between the anterior and posterior iris surfaces. Mathematically, this amounted to counting all the voxels enclosed within this space. The dimensions of each voxel are shown in Figure 4 (available at www.aaojournal.org). On the basis of these dimensions, the volume of each voxel is θr pixel^3, where θ is the angle between successive cross-sections and r is the distance of the voxel from the center of the pupil. In this study, $\theta = \pi/128$ (i.e., analysis was performed every 1.4°). By substituting for the value of θ and summing the volumes of all contributing voxels, we get iris volume to be $\pi/128 \sum_{s=1}^{128} \sum_{i=1}^{n} r_{si}(scaling\ factor)^3$, where s denotes the B-scan number (1−128), i denotes the A-scan number, and n is the number of A-scans within each B-scan that fall within the iris. The scaling factor was 9.7 μm/pixel. In a minority of images (1.6%), manual adjustments were made if the software failed to automatically detect the iris and corneal boundaries at the correct location. Pupil diameter (PD) was measured using our program, defined as the mean distance between the 2 pupil edges across all 128 cross-sectional scans.

Validation and Agreement of Iris Volume Measurements

Our measurement of iris volume was validated against an iris phantom of known volume (Fig 5, available at www.aaojournal.org). Briefly, we made the iris phantom by creating a computer-aided design model on the modeling software SolidWorks (Dassault Systemes SolidWorks Corporation, Waltham, MA) and built it using a 3D printer (Objet260 Connex3, Stratasys, Eden Prairie, MN) (Fig 5A, available at www.aaojournal.org). This iris phantom model was then scanned on the Casia SS-OCT machine (Fig 5B, available at www.aaojournal.org), and the iris volume obtained based on our methodology was compared with the actual volume of the model. We found the 2 volume measurements to be within 1% of each other.

A pilot study was performed on 20 randomly selected eyes to evaluate the agreement of iris volume measurements between automatic detection of iris boundaries by our customized program and semiautomatic detection of the iris boundaries by the built-in SS-OCT software (with the end points determined on the basis of scleral spur markings by an expert grader). The results showed that there was a high interobserver repeatability in terms of Pearson's R of 0.96 and intraclass correlation coefficients of 0.95 (95% confidence interval [CI], 0.89−0.98) (Fig 6, available at www.aaojournal.org). By comparing the change in iris volume from light to dark conditions on a set of 10 eyes, we obtained a Pearson's correlation of 0.83 and intraclass correlation coefficients of 0.75 (95% CI, 0.64−0.94).

Statistical Analysis

All baseline values were defined as those under bright lighting conditions. The primary outcome variable was the change in iris volume from light to dark conditions. The association between iris surface features (independent variables) and change in iris volume (dependent variable) was assessed by linear regression models. We included each iris surface feature one at a time and adjusted for other covariates in the linear regression models. Multivariable linear regression analysis was performed to assess the effect of each iris surface feature variable on change in iris

volume, adjusting for age and gender. In addition, the regression models were further adjusted for factors with biologically plausible relations to iris surface features or changes in iris volume, including the presence of corneal arcus and change in pupil size between light and dark conditions. Previous studies reported that change in pupil size between light and dark conditions was significantly related to change in iris volume.[5,6,8,9] Therefore, we included change in pupil size as a potential confounder in our regression analyses. Corneal arcus might make the iris color appear lighter on the iris photographs and might partially or completely block the view of the peripheral iris. We had earlier excluded eyes with extensive corneal arcus. To account for eyes with mild to moderate corneal arcus, we included the presence of corneal arcus in our multivariable regression models as a covariate to account for its potential effect on iris grading. In our analysis of baseline iris volume (i.e., in light condition), we also included pupil size from the SS-OCT images taken in light as a potential confounder, because it is directly proportional to iris thickness[26]; a larger pupil indicates more contraction of the iris in response to darkness, which will make the iris thicker. There was a strong correlation between the inter-eye difference in the iris volume ($r = 0.90$, $P < 0.001$). Data from the right eyes were used for analysis to eliminate an inter-eye correlation issue. Analysis was performed using STATA 12.1 (StataCorp LP, College Station, TX).

Results

Of the 86 Chinese participants recruited for the study, 5 were excluded because of poor-quality SS-OCT images in at least 1 quadrant, 5 were ungradable for furrows because of marked or extensive corneal arcus covering 50% or more of the entire iris area, and 11 had narrow angles (i.e., AOD 750 <225 μm).[23] In total, 65 (75.6%) open-angle participants had gradable data for crypts, furrows, and color, and were included in the analysis.

The demographics and ocular characteristics of the study participants are shown in Table 1. The mean (±standard deviation) age of the study participants was 59.8±5.7 years, and 64.6% were female (n = 42). On average, pupils of the study eyes enlarged 1.1 mm (range, 0.3−2.4 mm) in the dark condition. The mean iris volume in light condition was 38.0 mm³, and all eyes showed a reduction in iris volume (range, 0.1−2.9 mm³) when moving from light to dark. There were more eyes with a lower grade of iris crypts (76.9% with grade ≤2) than those with a higher grade (23.1% with grade ≥3). There were no eyes with iris crypt grade 5 (Fig 7, available at www.aaojournal.org). The distribution of iris furrows showed a different pattern; only 35.4% of eyes had a grade of 1. Iris color, measured using the CIE L* color parameter, was 29.6±6.4 (range, 19.5−45.5).

Table 2 shows the association between the 3 iris surface features and iris volume, namely, iris volume in light condition and change in iris volume moving from light to dark condition. In light condition, eyes with a higher crypt grading had a significantly smaller iris volume after controlling for age and gender (change in iris volume in millimeter per crypt grade increment, $\beta = -1.30$; 95% CI, −2.13 to −0.47; $P = 0.003$) (Table 2). The association ($\beta = -1.43$, 95% CI, −2.26 to −0.59; $P = 0.001$) was stronger in the model where age, gender, corneal arcus, and pupil size in light condition were included as covariates (Table 2).

Baseline iris volume was not significantly related to change in iris volume ($\beta = -0.05$; 95% CI, −0.10 to 0.00; $P = 0.051$, adjusting for age and gender). The change in pupil size between light and dark conditions was significantly related to change in iris

Table 1. Demographics and Baseline Characteristics of Chinese Participants Included in the Study (n = 65)

Characteristics	Mean (SD) or No. (%)
Age, yrs	59.84 (5.67)
Gender	
Male	23 (35.38)
Female	42 (64.62)
Corneal arcus	
No	36 (55.38)
Mild or moderate	29 (44.62)
Intraocular pressure, mmHg	14.34 (2.76)
Vertical cup-to-disc ratio	0.37 (0.10)
AOD, mm	0.41 (0.13)
Pupil diameter, mm	
Light	2.79 (0.60)
Dark	3.92 (0.79)
Change (light to dark)	−1.13 (0.48)
Iris volume, mm³	
Light	38.00 (3.56)
Dark	36.81 (3.79)
Change (light to dark)	1.19 (0.66)
Iris crypt	
Grade 1	30 (46.15)
Grade 2	20 (30.77)
Grade 3	12 (18.46)
Grade 4	3 (4.62)
Grade 5	0 (0)
Iris furrow	
Grade 1	23 (35.38)
Grade 2	30 (46.15)
Grade 3	12 (18.46)
Iris color* (0, dark; 100, light)	29.61 (6.44)

AOD = angle opening distance; SD = standard deviation.
*0 represents dark iris, and 100 represents light iris.

volume, after adjusting for age and gender ($\beta = 0.67$; 95% CI, 0.35−1.00; $P < 0.001$). Eyes with a higher crypt grading lost significantly more iris volume under dark conditions, after adjusting for age and gender ($\beta = 0.29$; 95% CI, 0.12−0.46; $P = 0.001$) (Table 2). After adjusting for confounders such as age, gender, cornea arcus, and change in pupil size, the association remained significant ($\beta = 0.23$; 95% CI, 0.06−0.40; $P = 0.010$) (Table 2). Figure 8 further illustrates the trend observed between iris crypt grades and iris volume as seen in the multivariable regression model. Eyes with a higher crypt grading had a significantly smaller iris volume (in light condition) (P trend = 0.001) (Fig 8A) and lost significantly more iris volume under dark conditions (P trend = 0.010) (Fig 8B). When we next considered volume change per millimeter of pupil dilation as an outcome measure, crypt grade was no longer statistically significant with volume change per millimeter of pupil dilation, after adjusting for age, gender, and corneal arcus ($\beta = 0.11$; 95% CI, −0.06 to 0.28; $P = 0.184$) (Fig 8C). Further analysis revealed that crypt grade was significantly associated with pupil enlargement. Specifically, eyes with a higher crypt grading exhibit a larger change in pupil size between light and dark, after adjusting for age and gender ($\beta = 0.18$; 95% CI, 0.06−0.30; $P = 0.004$) (Fig 8D). Therefore, the significance between crypt grade and volume change per millimeter of pupil dilation may effectively be nullified because the crypt grade is significantly correlated with changes in both iris volume and pupil enlargement.

Table 2. Associations of Iris Volume with Iris Crypt, Furrow, and Color

	Model 1*		Model 2†	
	β (95% CI)	P Value	β (95% CI)	P Value
Iris volume in light condition				
Crypt	−1.30 (−2.13 to −0.47)	**0.003**	−1.43 (−2.26 to −0.59)	**0.001**
Furrow	0.36 (−0.74 to 1.47)	0.515	0.23 (−0.98 to 1.44)	0.702
Color	−0.06 (−0.19 to 0.07)	0.357	−0.05 (−0.18 to 0.08)	0.465
Change in iris volume (light to dark)				
Crypt	0.29 (0.12−0.46)	**0.001**	0.23 (0.06−0.40)	**0.010**
Furrow	0.01 (−0.23 to 0.24)	0.967	−0.14 (−0.36 to 0.29)	0.222
Color	0.02 (−0.01 to 0.05)	0.196	0.01 (−0.02 to 0.03)	0.568

CI = confidence interval.
Bold values indicate significant differences of $P < 0.05$.
Each iris surface feature was included one at a time and adjusted for other covariates in the multivariable linear regression models. For example, the equation for crypts in Model 1 for change in iris volume as the outcome variable is *Changes in iris volume* $= \beta_0 + \beta_1{}^*crypt + \beta_2{}^*age + \beta_3{}^*gender$, where β_1 (i.e., β shown in the Table) is the estimated change in iris volume (in millimeters^3) for 1 grade higher in iris crypt, without furrow and color as covariates.
*Model 1: adjusted for age and gender.
†Model 2: For iris volume in light condition, β was adjusted for age, gender, corneal arcus, and pupil size in light (measured from SS-OCT). For change in iris volume, β was adjusted for age, gender, corneal arcus, and change in pupil size between light and dark conditions (measured from SS-OCT).

Iris furrows and color were not significantly associated with iris volume in light condition or dynamic iris volume change on pupil dilation both before and after adjustment for relevant confounders (all $P > 0.05$) (Table 2).

Discussion

In this study in Chinese persons, we found that some iris surface features were correlated with changes in iris volume during physiologic pupil dilation. Specifically, eyes with fewer iris crypts had larger iris volume under bright light condition and less reduction in iris volume during pupil dilation compared with those with more crypts. Other features (furrow and color) were not related to changes in iris volume. Therefore, our results suggest that iris crypt is an important factor, independent from iris color, that influences the responses of iris volume to varying illumination.

Iris regions containing crypts have a larger surface area, which might enhance fluid movement across the anterior surface of the iris. Other possible factors that might affect fluid movement through the iris include the proportion of iris that contains water, the degree to which water is bound by forces (i.e., hydrogen bonding), and the density of the iris stromal connective tissue. That is, crypts also could be surrogate for iris stroma characteristics. Specifically, we speculate that eyes with a higher crypt grading might represent stroma tissue that is relatively more compressible, that is, higher water content and less dense stroma iris tissues. Therefore, such eyes will have better fluid exchange and thus greater reduction on iris volume on pupillary dilation, which has been shown to be at a lesser risk of acute angle-closure attacks.[11,27] Further studies are needed to investigate whether crypts can increase fluid exchange sufficiently by iris surface area change alone or is indeed a surrogate for stromal tissue characteristics.

In our earlier report, we observed that eyes of Asian individuals with fewer crypts tend to have thicker irises.[14] Because fewer crypts are associated with less iris volume loss, one may expect that thicker irides lose less volume. However, in our study, a thicker iris (i.e., larger iris volume) does not lose less volume, suggesting the dominant factor mediating volume change is crypt number rather than iris thickness. Moreover, Seager et al[8] reported that Europeans had a relatively larger iris area, but a greater tendency to lose more iris area with dilation compared with Chinese persons. European eyes differ from Asian eyes in that they have more distinct crypts[17,18]; therefore, the presence of multiple larger crypts in European eyes may have contributed to the greater iris volume reduction in their study.

Previous studies have investigated the differential relationship between iris volume change and various types of angle closure (from suspects to glaucoma).[6–8,28] Seager et al[8] reported that the fellow eye of an eye with previous acute primary angle closure (PAC) exhibits greater retention of iris area as the pupil widens than primary angle-closure suspects. Others have confirmed that fellow eyes with acute PAC lose less iris area on pupil dilation than persons with PAC/PACG.[6,7] Lee et al[28] found no difference in the loss of iris area on dilation between patients with PAC/PACG and control normal Korean subjects. However, they excluded acute attack eyes. We speculate that such differences in iris dynamic behaviors between the various forms of angle closure may be due to the presence of visible crypts. On physiologic pupil dilation, the iris volume decreased, and the change was significantly more marked in eyes with a higher iris crypt grade. Because crypt grade is significantly correlated with both changes in iris volume and pupil enlargement, the parameter of volume change per millimeter of pupil dilation may not effectively demonstrate the relationship between crypt grade and dynamic iris volume change. The correlation between higher crypt grades and greater change in pupil size correspondingly suggests that crypt grade could be a proxy measure of a more compressible type of iris stroma that can allow greater pupil enlargement (as well as greater reduction in iris volume). In contrast to studies that used volume change per millimeter pupil dilation as a clinical parameter, our intention is to use the iris crypt grade to identify patients at risk of angle closure. Such an inherent functional characteristic of fluid retention also has been linked to eyes predisposed to acute angle-closure attack,[29] suggesting that the presence of iris crypts may be used to predict which eyes with anatomically narrow angles are at a greatest risk of acute angle closure attack. Longitudinal studies on narrow-angle eyes are needed to establish whether iris crypts could directly predict the occurrence and progression of angle-closure glaucoma.
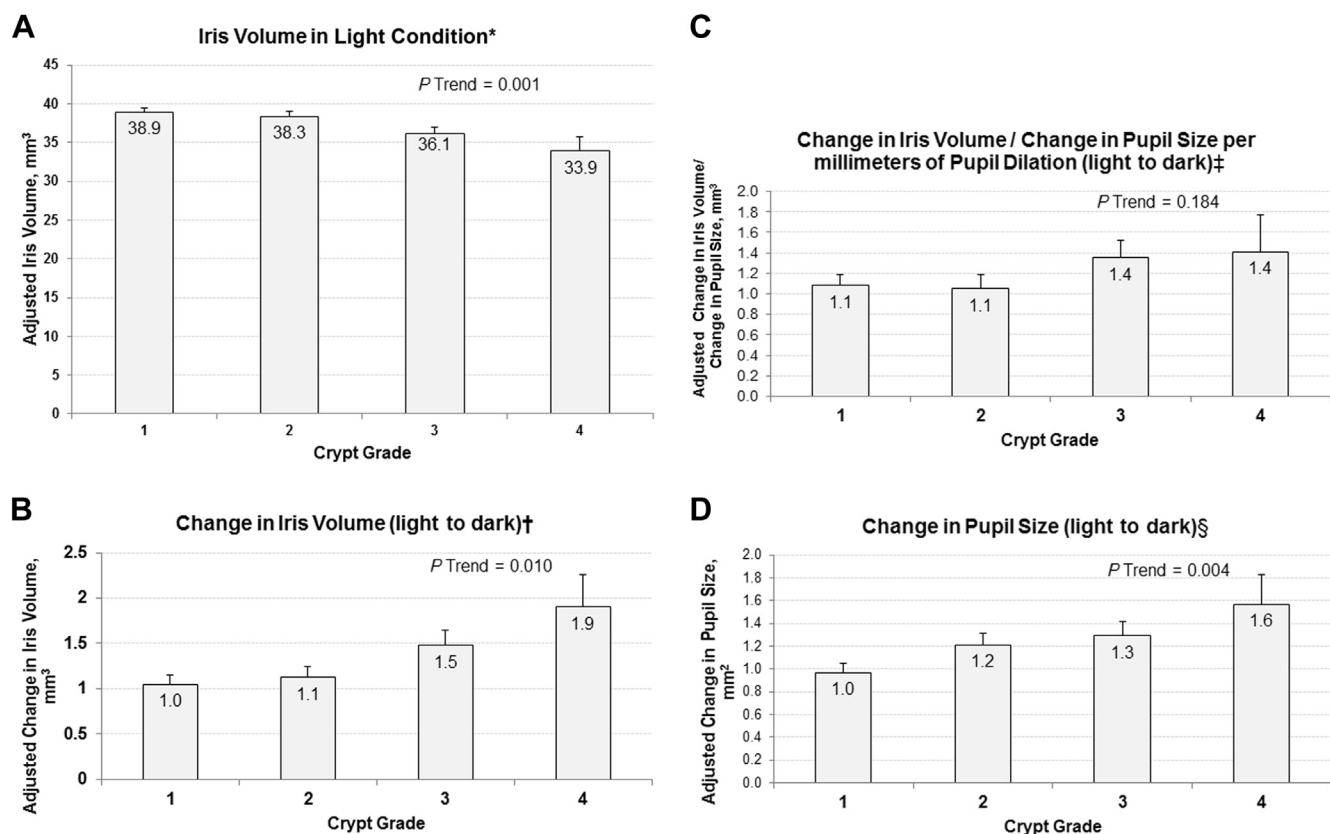
A

B

C

D

Figure 8. Distribution of (**A**) iris volume in light condition, (**B**) change in iris volume, (**C**) change in iris volume/change in pupil size per millimeters of pupil dilation, and (**D**) change in pupil size stratified by iris crypt grades. *Data and *P* values shown are after adjustment for age, gender, corneal arcus, and pupil size in light condition. [†]Data and *P* values shown are after adjustment for age, gender, corneal arcus, and change in pupil size. [‡]Data and *P* values shown are after adjustment for age, gender, and corneal arcus. [§]Data and *P* values shown are after adjustment for age and gender.

The varying shades of coloration at the iris surface are determined by 2 major components, namely, the amount of melanin in the iris or the arrangement of melanosomes in the pigment epithelial cells, and the light-scattering properties of the iris tissue.[12,30] Clinical assessment of iris color commonly is used in studies to assess an individual's iris melanin content.[5,6,8] However, assigning each individual to a specific color is challenging and prone to information bias. The current study measures iris color from photographs, based on CIE L* color parameter, allowing for a more objective method of quantifying iris color, and thereby providing a more accurate and reliable comparison of the iris color among various brown-eyed Asians. Nevertheless, we did not observe a significant association between iris color and dynamic iris volume change on pupil dilation, possibly because the irides in our Chinese population are almost exclusively brown in color, and the variation in color within the Asian ethnicity is small.

Studies examining iris color and the dynamic changes of iris volume have provided conflicting results. Aptel and Denis[6] investigated the dynamic iris change in Europeans and observed that subjects with brown eyes had a relatively smaller change in iris volume than those with blue eyes. This may seem plausible considering the fact that a darker iris may have thicker peripheral iris,[14] possibly because of the higher melanin content, which also may contribute to larger irides and less change in volume with dilation. However, the majority of their European subjects (80%) had brown eyes, whereas only 20% had blue eyes.[6] Other studies have observed no association between dynamic iris change and iris color.[5,8] Quigley et al[5] and Seager et al[8] demonstrated that European-derived and African-derived persons exhibited similar dynamic iris area change. Therefore, European-derived persons with their lighter irides did not have a greater loss of iris area than African-derived persons (darker irides). We speculate that ethnic disparities of iris dynamic behaviors seen in previous studies are likely to be independent of iris color; rather, they are due to the presence of visible crypts. Asian eyes differ from European eyes in that they have fewer distinct crypts,[17,18] despite comparable ocular biometric profiles.[31]

Traditionally, scleral spurs had to be manually detected to measure both iris area and volume.[6,8,9,11] Moreover, studies have reported that scleral spurs cannot be identified in 15% to 28% of AS-OCT images,[3,32] and their identification has been subject to measurement error and variability.[33,34] In addition, Seager et al[25] showed that the iris area measurement is not affected by the precision of the scleral spur marked position. We circumvented these issues by developing an automated method to provide the iris volume from the iris area measurements, without the manual identification of

scleral spurs. Apart from making the measurement process rapid and efficient, we demonstrated high interobserver repeatability that indicated the robustness of the software. Without the manual input of scleral spurs, this validated measurement technique can allow investigators to efficiently calculate the iris area and thus dynamic iris volume changes in a larger scale.

Previous studies have found that the iris volume increased in eyes with acute angle-closure attack compared with controls.[6,7,11] However, Seager et al[8] demonstrated that such an "increase" of iris volume is an artifact of the calculation. Because angle-closure eyes were more likely to redistribute their peripheral iris area than controls, producing a more peripheral center of iris mass (centroid), the use of the centroid to calculate the iris volume has inadvertently introduced a bias. Our novel yet simplified calculation method allows researchers to derive the iris volume without the input of the centroid.

Study Strengths and Limitations

Strengths of the study include the use of SS-OCT to measure iris volume. Compared with conventional AS-OCT, SS-OCT allows 360° imaging of the iris and thus provides a global assessment of iris volume. The limitations of the study include a relatively small number of participants with higher iris crypt grade, especially grade 4 and none with grade 5. Second, all study subjects were Chinese, and thus we are not able to compare the difference in associations between ethnic groups. Our results may not be directly applied to people of European ancestry, whose eyes have a higher crypt frequency[12,13] and lighter color than Asian eyes.[35,36] Third, all of our participants had normal open angles. Further investigation of the dynamic iris response with AS-OCT in people with different angle-closure stage is needed to assess how iris crypts could affect iris volume change in angle-closure diseases. Last, our results were obtained after physiologic mydriasis. We chose this method because it reflects the natural state of pupil activity. In further work, it will be interesting to perform similar investigations after pharmacologic pupil dilation.

In conclusion, we have found in Chinese persons that eyes with fewer iris crypts had larger iris volume and exhibited less loss of iris volume after physiologic pupil dilation than those eyes with more iris crypts. Iris furrows and varying shades of brown color at the iris surface were not related to the iris volume in light condition or changes of iris volume. Our study suggests the need for quantitative assessment of iris crypts in studies assessing iris dynamics with various types of angle closure. Our findings also highlight the importance of iris crypts on iris dynamics and angle-closure pathogenesis and their possible future use as a clinical predictive test for angle closure.

References

1. Tham YC, Li X, Wong TY, et al. Global prevalence of glaucoma and projections of glaucoma burden through 2040: a systematic review and meta-analysis. Ophthalmology 2014;121:2081–90.
2. Wang B, Sakata LM, Friedman DS, et al. Quantitative iris parameters and association with narrow angles. Ophthalmology 2010;117:11–7.
3. Wang BS, Narayanaswamy A, Amerasinghe N, et al. Increased iris thickness and association with primary angle closure glaucoma. Br J Ophthalmol 2011;95:46–50.
4. Ishikawa H, Liebmann JM, Ritch R. Quantitative assessment of the anterior segment using ultrasound biomicroscopy. Curr Opin Ophthalmol 2000;11:133–9.
5. Quigley HA, Silver DM, Friedman DS, et al. Iris cross-sectional area decreases with pupil dilation and its dynamic behavior is a risk factor in angle closure. J Glaucoma 2009;18:173–9.
6. Aptel F, Denis P. Optical coherence tomography quantitative analysis of iris volume changes after pharmacologic mydriasis. Ophthalmology 2010;117:3–10.
7. Narayanaswamy A, Zheng C, Perera SA, et al. Variations in iris volume with physiologic mydriasis in subtypes of primary angle closure glaucoma. Invest Ophthalmol Vis Sci 2013;54:708–13.
8. Seager FE, Jefferys JL, Quigley HA. Comparison of dynamic changes in anterior ocular structures examined with anterior segment optical coherence tomography in a cohort of various origins. Invest Ophthalmol Vis Sci 2014;55:1672–83.
9. Mak H, Xu G, Leung CK. Imaging the iris with swept-source optical coherence tomography: relationship between iris volume and primary angle closure. Ophthalmology 2013;120:2517–24.
10. Friedman DS, Gazzard G, Foster P, et al. Ultrasonographic biomicroscopy, Scheimpflug photography, and novel provocative tests in contralateral eyes of Chinese patients initially seen with acute angle closure. Arch Ophthalmol 2003;121:633–42.
11. Aptel F, Chiquet C, Beccat S, et al. Biometric evaluation of anterior chamber changes after physiologic pupil dilation using Pentacam and anterior segment optical coherence tomography. Invest Ophthalmol Vis Sci 2012;53:4005–10.
12. Larsson M, Pedersen NL. Genetic correlations among texture characteristics in the human iris. Mol Vis 2004;10:821–31.
13. Spierer A, Isenberg SJ, Inkelis SH. Characteristics of the iris in 100 neonates. J Pediatr Ophthalmol Strabismus 1989;26:28–30.
14. Sidhartha E, Gupta P, Liao J, et al. Assessment of iris surface features and their relationship with iris thickness in Asian eyes. Ophthalmology 2014;121:1007–12.
15. Sidhartha E, Nongpiur ME, Cheung CY, et al. Relationship between iris surface features and angle width in Asian eyes. Invest Ophthalmol Vis Sci 2014;55:8144–8.
16. Rukmini AV, Milea D, Baskaran M, et al. Pupillary responses to high-irradiance blue light correlate with glaucoma severity. Ophthalmology 2015;122:1777–85.
17. Foster PJ, Buhrmann R, Quigley HA, et al. The definition and classification of glaucoma in prevalence surveys. Br J Ophthalmol 2002;86:238–42.
18. Weatherall IL, Coombs BD. Skin color measurements in terms of CIELAB color space values. J Invest Dermatol 1992;99:468–73.
19. Takiwaki H. Measurement of skin color: practical application and theoretical considerations. J Med Invest 1998;44:121–6.
20. Alaluf S, Heinrich U, Stahl W, et al. Dietary carotenoids contribute to normal human skin color and UV photosensitivity. J Nutr 2002;132:399–403.

21. Liu S, Yu M, Ye C, et al. Anterior chamber angle imaging with swept-source optical coherence tomography: an investigation on variability of angle measurement. Invest Ophthalmol Vis Sci 2011;52:8598–603.
22. Pavlin CJ, Harasiewicz K, Foster FS. Ultrasound biomicroscopy of anterior segment structures in normal and glaucomatous eyes. Am J Ophthalmol 1992;113:381–9.
23. Narayanaswamy A, Sakata LM, He MG, et al. Diagnostic performance of anterior chamber angle measurements for detecting eyes with narrow angles: an anterior segment OCT study. Arch Ophthalmol 2010;128:1321–7.
24. Aptel F, Chiquet C, Gimbert A, et al. Anterior segment biometry using spectral-domain optical coherence tomography. J Refract Surg 2014;30:354–60.
25. Seager FE, Wang J, Arora KS, et al. The effect of scleral spur identification methods on structural measurements by anterior segment optical coherence tomography. J Glaucoma 2014;23: e29–38.
26. Wang D, He M, Wu L, et al. Differences in iris structural measurements among American Caucasians, American Chinese and mainland Chinese. Clin Experiment Ophthalmol 2012;40:162–9.
27. Quigley HA. The iris is a sponge: a cause of angle closure. Ophthalmology 2010;117:1–2.
28. Lee Y, Sung KR, Na JH, et al. Dynamic changes in anterior segment (AS) parameters in eyes with primary angle closure (PAC) and PAC glaucoma and open-angle eyes assessed using AS optical coherence tomography. Invest Ophthalmol Vis Sci 2012;53:693–7.
29. Quigley HA, Friedman DS, Congdon NG. Possible mechanisms of primary angle-closure and malignant glaucoma. J Glaucoma 2003;12:167–80.
30. Imesch PD, Bindley CD, Khademian Z, et al. Melanocytes and iris color. Electron microscopic findings. Arch Ophthalmol 1996;114:443–9.
31. Congdon NG, Youlin Q, Quigley H, et al. Biometry and primary angle-closure glaucoma among Chinese, white, and black populations. Ophthalmology 1997;104:1489–95.
32. Sakata LM, Lavanya R, Friedman DS, et al. Assessment of the scleral spur in anterior segment optical coherence tomography images. Arch Ophthalmol 2008;126:181–5.
33. Leung CK, Yung WH, Yiu CK, et al. Novel approach for anterior chamber angle analysis: anterior chamber angle detection with edge measurement and identification algorithm (ACADEMIA). Arch Ophthalmol 2006;124:1395–401.
34. Li H, Leung CK, Cheung CY, et al. Repeatability and reproducibility of anterior chamber angle measurement with anterior segment optical coherence tomography. Br J Ophthalmol 2007;91:1490–2.
35. Edwards M, Gozdzik A, Ross K, et al. Technical note: quantitative measures of iris color using high resolution photographs. Am J Phys Anthropol 2012;147:141–9.
36. Sturm RA, Larsson M. Genetics of human iris colour and patterns. Pigment Cell Melanoma Res 2009;22:544–62.

Footnotes and Financial Disclosures

[1] Singapore Eye Research Institute, Singapore National Eye Centre, Singapore.

[2] Ophthalmology and Visual Sciences Academic Clinical Program, Duke-NUS Medical School, Singapore.

[3] Department of Biomedical Engineering, National University of Singapore, Singapore.

[4] Department of Ophthalmology, Yong Loo Lin School of Medicine, National University of Singapore and National University Health System, Singapore.

[5] SingHealth Polyclinics, Outram, Singapore.

Abbreviations and Acronyms:

AOD = angle opening distance; **AS-OCT** = anterior-segment optical coherence tomography; **CI** = confidence interval; **CIE** = Commission Internationale de l'Eclairage; **PAC** = primary angle closure; **PACG** = primary angle-closure glaucoma; **SS-OCT** = swept-source optical coherence tomography; **3D** = 3-dimensional.

Correspondence:
Ching-Yu Cheng, MD, PhD, The Academia, 20 College Road, Level 6, Discovery Tower, Singapore 169856. E-mail: chingyu.cheng@duke-nus.edu.sg.